AGU PUBLICATIONS

JGR

Journal of Geophysical Research: Biogeosciences

RESEARCH ARTICLE

10.1002/2016JG003387

Key Points:
- CH_4 formed in saturated soils above permafrost can influence surface water CH_4 budgets via soil water discharge
- We show novel data on redox dynamics and CH_4 in hillslope permafrost soils and the potential for transport to streams
- Hillslope soils become anoxic as thaw deepens and CH_4 content increases but we find no evidence of a link to stream CH_4

Supporting Information:
- Supporting Information S1

Correspondence to:
L. E. Street,
lorna.street@ed.ac.uk

Citation:
Street, L. E., J. F. Dean, M. F. Billett, R. Baxter, K. J. Dinsmore, J. S. Lessels, J.-A. Subke, D. Tetzlaff, and P. A. Wookey (2016), Redox dynamics in the active layer of an Arctic headwater catchment; examining the potential for transfer of dissolved methane from soils to stream water, *J. Geophys. Res. Biogeosci.*, *121*, 2776–2792, doi:10.1002/2016JG003387.

Received 18 FEB 2016
Accepted 7 OCT 2016
Accepted article online 12 OCT 2016
Published online 5 NOV 2016

Redox dynamics in the active layer of an Arctic headwater catchment; examining the potential for transfer of dissolved methane from soils to stream water

Lorna E. Street[1,2], Joshua F. Dean[3,4], Michael F. Billett[3], Robert Baxter[5], Kerry J. Dinsmore[6], Jason S. Lessels[7], Jens-Arne Subke[3], Doerthe Tetzlaff[7], and Philip A. Wookey[1]

[1]School of Life Sciences, Heriot-Watt University, Edinburgh, UK, [2]School of GeoSciences, University of Edinburgh, Edinburgh, UK, [3]Biological and Environment Sciences, School of Natural Sciences, University of Stirling, Stirling, UK, [4]Earth and Climate Cluster, Faculty of Earth and Life Sciences, Vrije Universiteit Amsterdam, Amsterdam, Netherlands, [5]Department of Biosciences, University of Durham, Durham, UK, [6]Centre for Ecology and Hydrology, Penicuik, UK, [7]Northern Rivers Institute, School of Geosciences, University of Aberdeen, Aberdeen, UK

Abstract The linkages between methane production, transport, and release from terrestrial and aquatic systems are not well understood, complicating the task of predicting methane emissions. We present novel data examining the potential for the saturated zone of active layer soils to act as a source of dissolved methane to the aquatic system, via soil water discharge, within a headwater catchment of the continuous permafrost zone in Northern Canada. We monitored redox conditions and soil methane concentrations across a transect of soil profiles from midstream to hillslope and compare temporal patterns in methane concentrations in soils to those in the stream. We show that redox conditions in active layer soils become more negative as the thaw season progresses, providing conditions suitable for net methanogenesis and that redox conditions are sensitive to increased precipitation during a storm event—but only in shallower surface soil layers. While we demonstrate that methane concentrations at depth in the hillslope soils increase over the course of the growing season as reducing conditions develop, we find no evidence that this has an influence on stream water methane concentrations. Sediments directly beneath the stream bed, however, remain strongly reducing at depth throughout the thaw season and contain methane at concentrations 5 orders of magnitude greater than those in hillslope soils. The extent of substreambed methane sources, and the rates of methane transport from these zones, may therefore be important factors determining headwater stream methane concentrations under changing Arctic hydrologic regimes.

1. Introduction

Surface waters in high-latitude permafrost regions act as hot spots of methane emissions [*Walter et al*., 2006; *Flessa et al*., 2008; *Bastviken et al*., 2011]. Lakes and ponds are estimated to account for two thirds of natural land surface methane sources in the boreal region northward [*Wik et al*., 2016]. Methane release from surface waters can occur via multiple pathways; as bubbles from deeper waters or sediments (ebullition) [*Baulch et al*., 2011; *Crawford et al*., 2014b], via transport through the tissues of aerenchymatous plants [*Le Mer and Roger*, 2001; *King and Reeburgh*, 2002] or as a result of diffusive release (degassing) of methane dissolved in the water column [*Kling et al*., 1992; *Billett and Moore*, 2008; *Dinsmore et al*., 2009]. Lakes and pond waters are often supersaturated with methane with respect to the atmosphere, and diffusive fluxes are a significant methane release pathway [*Kling et al*., 1992; *Knoblauch et al*., 2015], although in lakes ebullition fluxes are usually larger [*Sepulveda-Jauregui et al*., 2015]. Stream systems have been much less well studied but can also act as conduits of methane to the atmosphere, thereby playing a potentially important role in catchment greenhouse gas budgets. For example, in boreal Alaska, methane efflux (primarily via diffusion) from a headwater stream network was estimated to account for up to 10% of terrestrial methane sources, despite accounting for $<$0.2% of the catchment surface area [*Crawford et al*., 2013]. Furthermore, the presence of high concentrations of dissolved methane in both lakes and streams has ecological significance as methane can support freshwater productivity via methanotrophic pathways [*Medvedeff and Hershey*, 2013; *Hershey et al*., 2015]. We understand very little, however, about the origins of dissolved methane in freshwaters; the mechanisms driving dissolved methane dynamics and the importance of linkages between terrestrial and aquatic systems; this is especially true for headwater catchments, where the role of terrestrial-freshwater coupling assumes particular significance [*Wrona et al*., 2016].

Transport of dissolved methane from soils into lakes and streams via shallow groundwater discharge has been implicated as an important source of methane to the aquatic system [*Kling et al*., 1992; *Jones and Mulholland*, 1998; *Crawford et al*., 2014a]. In their Alaskan study, *Crawford et al*. [2013] identified regions of the stream which were consistently elevated in methane concentrations, implying an important role for discreet inflows of methane-rich groundwater. It is reasonable to expect that the transfer of methane from terrestrial sources to the aquatic system may be particularly important in permafrost regions, where the presence of permafrost gives rise to a carbon-rich water-saturated zone which can provide conditions favorable to methane production [*Treat et al*., 2015]. For example, in an Alaskan lake, discharge of methane-enriched soil water from surrounding active layer soils has been shown to significantly influence methane concentrations in the lake water [*Paytan et al*., 2015]. The potential importance of dissolved methane sources and transport pathways for headwater stream systems in permafrost regions is still largely unknown, but this knowledge is important for our understanding of the functioning of freshwater systems and their role as methane emission hotpots under a future Arctic climate. Understanding the role of terrestrial sources in aquatic methane budgets is challenging, however, because it requires both an understanding of potential source areas within the landscape and the transport processes operating at the terrestrial-freshwater interface.

Biological processing of organic matter is dominated by redox reactions, and soil redox potential (Eh) is a critical environmental control over methanogenesis [*Husson*, 2012]. The presence of a saturated soil zone above permafrost can potentially result in the strongly reducing conditions necessary for methane production [*Peters and Conrad*, 1996]; however, the relationship between soil moisture content and redox potential is complex [*McNicol and Silver*, 2014]. It takes time for oxygen to be depleted, and input of oxygenated water via precipitation or lateral flow can prevent reducing conditions from developing [*Hall et al*., 2012]. In wetland systems water table position is the primary factor controlling soil redox states [*Kettunen et al*., 1999; *Seybold et al*., 2002]; however, if lateral flows dominate catchment hydrology, then soil redox potential and water table depth become decoupled [*Mitchell and Branfireun*, 2005]. In permafrost regions there is very little understanding of redox dynamics associated with the seasonal development of the thaw front, in spite of its obvious significance for biogeochemical processing and patterns of methane production [*Lipson et al*., 2015]. Time series (or indeed any) data on the redox status of Arctic soils and sediments are rarely available. Changes in dominant hydrological processes associated with climate change and deepening of the active layer [*Tetzlaff et al*., 2015] may alter redox conditions in permafrost soils and subsequent delivery of methane to the aquatic system, so it is important to understand hillslope redox dynamics and how they relate to redox-sensitive biogeochemical processes.

The lack of available data to quantify temporal and spatial patterns in soil redox potentials in permafrost systems is likely the result of a combination of the logistical challenges of working in remote regions and a view among researchers that soil redox potential measurements are only semiquantitative. This criticism arises from important difficulties involved in interpreting redox potential data. These limitations have been reviewed in detail elsewhere [*Grundl*, 1994; *Fiedler et al*., 2007], but we highlight here two key points which complicate data interpretation:

1. In ideal chemical systems (i.e., in pure solutions at low ionic strength), the redox potential for any particular redox couple is determined by the activities (concentrations) of each reactant via the Nernst equation [*Skoog et al*., 1996]. Soils, however, are a complex, spatially heterogeneous mixture of multiple redox couples in both solid and liquid phases, at unknown activities and at chemical disequilibrium [*Grundl*, 1994]. As a result, redox potentials cannot be interpreted in a quantitative way based on thermodynamic principles, and this includes standardizing measured Eh values for soil pH and temperature (empirical relationships between soil pH and redox potential have been developed across a variety of soil types and a correction factor of −59 mV per unit of pH change has been proposed, but this correction is not necessarily applicable to soils with high pH buffering capacity [*Sparks*, 2003]).
2. The spatial heterogeneity of soils means there may be nearby microsites within the soil structure which are at a very different potential to the point of measurement [*Parkin*, 1987; *Teh and Silver*, 2006]. Both of these factors make it difficult to define exact Eh thresholds at which any particular biogeochemical reaction will or will not occur, but redox potentials can be used to examine the spatial and temporal patterns in the degree to which soils are oxidizing or reducing, the drivers of those patterns, and the linkages to biogeochemical properties within the system of interest (in this case, permafrost catchments) [*Fiedler and Sommer*, 2000; *Fiedler et al*., 2007].

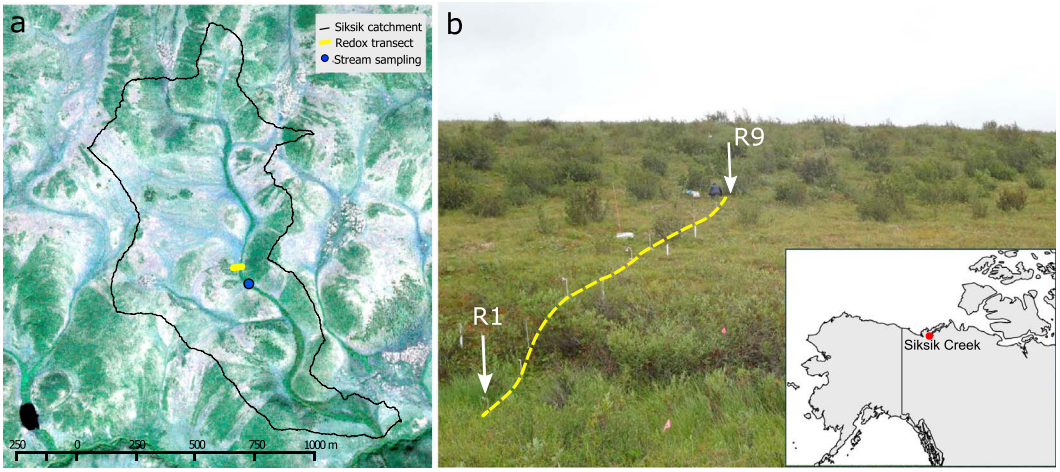

Figure 1. Images of the study site (a) satellite image of Siksik creek catchment with redox measurement transect and stream sampling locations; (b) photograph of the redox measurement transect. R1 indicates the location of the redox probe in the middle of the stream channel, R9 the probe at the farthest point from the stream; the inset shows the location of study site in NW Canada.

Here we present findings of a study examining how seasonal deepening of the thaw front and changes in hydrological conditions influence soil redox potentials and the concentrations of methane in the soils and stream of an Arctic headwater catchment. The overall aim of the study was to understand the role of soil redox dynamics in determining conditions for methanogenesis and the subsequent potential for delivery of dissolved methane in active layer soil water from soils to stream waters. We address the following specific questions: (1) How do redox conditions in hillslope soils vary through the thaw season as the active layer deepens? (2) To what degree are redox potentials in soils related to soil methane concentrations? and (3) To what extent are changing soil redox conditions linked to instream redox dynamics and aquatic methane concentrations? We expect that reducing conditions, which develop in saturated soils above the active layer, are associated with methane generation and that methane present at depth in hillslope soils adjacent to the stream channel can impact stream water methane concentrations via discharge of active layer soil water.

2. Methods

2.1. Site Description

The study was carried out in the Siksik Creek catchment (68°44′54.5″N, 133°29′41.7″W), approximately 55 km north-northeast of Inuvik, NWT, Canada (Figure 1). Siksik Creek is a first-order stream flowing north to south with a total catchment area of 0.94 km^2 and is a tributary of Trail Valley Creek, which flows into the Husky Lakes saltwater regions to the east. The mean elevation of the site is ~80 m above sea level, with approximately 30 m difference in altitude between the stream channel and hill tops. The transect established to measure redox potentials in the soil profile (see section 2.2) was located in the middle of the catchment, with a subcatchment area of ~0.53 km^2. The transect was located in a midcatchment position sufficiently far upstream of the preestablished water sampling site to avoid disturbance. Based on observation of the surrounding vegetation and topography, we had no reason to believe that the location was atypical in comparison to other nearby midcatchment positions.

The study catchment is in the continuous permafrost zone of the western Canadian Arctic. Mean air temperatures were −16.7°C for October 2013 to April 2014, and 7.1°C for May to September 2014; similar to the mean monthly temperatures in the region of 7.7°C (±1.1σ) from May to September and −20.9°C (±2.1σ) from October to April [*Teare*, 1998]. Precipitation in 2014 was 277 mm, similar to mean annual precipitation from 1960 to 2005 [*Marsh et al.*, 2002]. The freshet, derived from spring snowmelt, dominates the hydrology of the area and comprises ~90% of annual flow [*Quinton and Marsh*, 1999]. The freshet commenced in late May in 2014, following an 8 month snow covered season, with deep snow beds remaining until mid-June.

Soils in the catchment are organic-rich cryosols, 0.05–0.5 m thick, overlying a 1 m thick Quaternary Pleistocene till layer which is underlain by unconsolidated chert, quartzitic sandstone and siltstone alluvial

Table 1. Soil pH, Depth of the Organic Horizon, Maximum Frost Table Depth, and Extent of the Saturated Soil Zone at Each Transect Position

Position	pH			O Horizon Depth (m)	Max Frost Table Depth (m) ±1σ		Mean Saturated Zone Extent (m)	
	0.1 m	0.2 m	0.3 m		Jul	Aug/Sep	Jul	Aug/Sep
R1	5.3	-	-	0.1–0.2[a]	0.78 ± 0.14	0.81 ± 0.17	-	-
R2	5.1	5.2	4.8	0.1–0.2[b]	0.62 ± 0.03	0.59 ± 0.05	-	-
R3	5.1	4.7	-	>0.35	0.32 ± 0.01	0.35 ± 0.03	0.00	0.00
R4	5.2	5.1	-	>0.41	0.33 ± 0.04	0.41 ± 0.07	0.09	0.11
R5	5.4	5.3	5.5	0.15	0.51 ± 0.04	0.57 ± 0.08	0.11	0.17
R6	4.5	5.0	4.7	0.14	0.48 ± 0.07	0.51 ± 0.05	0.14	0.24
R7	5.4	5.3	5.3	0.20	0.50 ± 0.03	0.57 ± 0.05	0.21	0.38
R8	5.2	5.6	5.0	0.11	0.52 ± 0.08	0.48 ± 0.04	0.17	0.28
R9	4.8	5.2	5.4	0.21	0.48 ± 0.03	0.44 ± 0.03	0.13	0.19

[a]O horizon between 0.1 and 0.2 m depth. Dense root mat to depth >0.5 m.
[b]O horizon between 0.1 and 0.2 m depth. Dense root mat to depth >0.3 m.

gravel of the Tertiary Beaufort Formation [*Rampton*, 1987; *Teare*, 1998]. The till layer is characterized by a heterogeneous hummock-interhummock morphology (0.4–1 m wide and 0.1–0.4 m high). The interhummock areas have deeper organic soils than the hummocks and dominate the hydrological response of the catchment following the freshet [*Quinton and Marsh*, 1998, 1999; *Quinton and Pomeroy*, 2006; *Quinton et al*., 2000]. The streambed is composed of the same till material as in the mineral hummocks, with organic-rich sediment deposits of 0.1–0.2 m in the stream channel (Table 1).

The vegetation is characterized by upland heath tundra, with lichens, prostrate *Salix* species, and ericaceous shrubs on the hill tops, and patches of dwarf birch (*Betula glandulosa*) and green alder (*Alnus viridis*) on the hillslopes. Bordering Siksik Creek (up to ~1–2 m width) is denser vegetation dominated by tall shrub growth forms including *B. glandulosa*, and *Salix* species; we refer to this area as the riparian zone. The area immediately adjacent to the riparian zone at the bottom of the hillslopes is often without shrubs and has high moss cover, including *Sphagnum* species (we refer to this as "channel bank"). Sedges (predominantly *Carex* spp.) are common within the riparian zone and the stream channel. Both stream water and soils in the catchment are low in mineral nutrient concentrations; nitrate N is below detection limit in Siksik Creek [*Dean et al*., 2016] and $<2\ \mu g\ g^{-1}$ in soils in green alder-dominated vegetation at the same site (L. Street, unpublished data, 2014).

2.2. Redox Potential Measurements

We established a 28 m long transect of nine sampling points (R1 in the stream channel to R9 farthest from the stream channel) running perpendicularly from the stream channel across the channel bank to a lower hillslope position within a large east facing patch of *A. viridis* (Figure 1). Hummock morphology is less well developed in the lower hillslope and channel bank areas. Redox potentials were measured using probes following the methods of *Vorenhout et al*. [2011]. The redox probes were 12 mm in diameter and constructed of fiberglass material with embedded platinum electrodes (Paleoterra, Amsterdam, Netherlands). The probes were inserted vertically into the soil; six probes were 0.4 m long in total and had redox electrodes at 0.02 m, 0.12 m, and 0.22 m from the probe tip, three probes were 0.6 m long, with redox sensors at 0.02 m, 0.22 m, 0.32 m, and 0.42 m from the tip. We inserted the probes in stages over the course of the thaw season as the permafrost thaw front deepened, such that electrodes were positioned at 0.1 m, 0.2 m, and 0.3 m depth for the shorter probes, and 0.1 m, 0.2 m, 0.3 m, and 0.5 m depth for the longer probes. This meant that the depth of measurement in the soil profile was kept constant (to the nearest centimeter), even though the specific electrode positioned at a particular depth changed at intervals during the season. The probe in the center of the stream channel was positioned such that one electrode measured the redox potential of the stream water 0.1 m above the stream bed surface. We did not install the probes the previous winter to avoid potential damage due to freeze-thaw effects and frost heave; they were instead installed on 12 June, early in the growing season, with measurements starting immediately. We used an Ag/AgCl reference electrode positioned at the midpoint of the transect at a depth of 0.2 m. This electrode is designed for permanent installation in soils and consists of a stable Ag/AgCl element surrounded by a solid electrolyte. A porous ceramic plug allows contact between the electrolyte and the soil (Type WE200, Silvion, Grantham, UK).

Redox potentials and temperatures were logged using a datalogger (CR800, Campbell Scientific, Logan, USA) connected to a 32-channel relay multiplexer (AM16/32B, Campbell Scientific, Logan, UK). Measurements were taken and stored every 10 min. Electron flow between electrodes during a redox potential measurement can result in drift effects as the proportion of oxidized and reduced species changes via reaction with the surface of the probe. However, if high measurement resistances are used, current flow is extremely low, and these effects can be minimized The input resistance of the datalogger was 20 GΩ, sufficient to prevent significant drift effects on soil redox potential when used in conjunction with a multiplexer, which maintains an open circuitry except during the period of measurement [*Rabenhorst et al*., 2009]. Data are expressed relative to a standard hydrogen electrode, but not corrected for temperature and pH. Eh is positive and high in oxidizing systems and low or negative in reducing conditions, and would be expected to decrease as pH increases. As detailed above, it is impossible to define an exact redox potential threshold at which methanogenesis will occur, but the range 0 to +300 mV is usually defined as "moderately reducing" conditions, in that electron acceptors other than O_2 begin to be utilized [*Fiedler et al*., 2007]. Within this range we choose to define "reducing conditions" as Eh $<$ +200 mV on the basis that [*Yu et al*., 2007] found the methane compensation point in soil (production = consumption) to be around +400 mV at pH 7, which is roughly equivalent to +240 mV at the minimum pH for our system. In reality, however, there is a gradient between "oxidizing" and "reducing" conditions in soils.

Redox sensors can function reliably in unsaturated soils, as long as adequate contact is maintained between the probe and the soil, and this is possible as long as soils are sufficiently moist. *Van Bochove et al*. [2002] demonstrate reliable redox measurements for soils with volumetric water content (VWC) between 0.20 $m^3\,m^{-3}$ and 0.29 $m^3\,m^{-3}$. We monitored the VWC of soils at 0.05 m depth at a nearby location on the stream bank (approximately 10 m from the redox probe measurements) using a HOBO ECH_2O soil moisture probe (Onset Inc, Pocasset,MA, USA). Data were recorded every 10 min using HOBO Micro-Station data loggers (Onset Inc). VWC measured by the moisture probes varied between ~0.2 and 0.5 $m^3\,m^{-3}$ over the measurement period (Figure S2 in the supporting information).

We tested the variability between the electrodes prior to installation by placing the probes in tap water. The tap water in the Inuvik area, where this testing was carried out, is sourced from a local lake and is therefore similar to soil solution in that it contains a complex mix of dilute redox couples at low concentrations. Our primary aim was to check that the probes were functioning as expected and to quantify consistency between probes. For the reasons outlined above, it is difficult to standardize redox potential measurements, so the absolute value of redox potential is not of primary importance. The average reading across all electrodes in tap water was +277 mV ± 7σ which is a typical value for tap water [*Goncharuk et al*., 2010], and the variability between probes was small in comparison to previously published data [*Fiedler et al*., 2007]. (Figure S1 in the supporting information). The electrode at 0.32 m from the tip on probe R1 was an outlier in this test and was also unresponsive to reducing conditions in the field (as indicated by the electrodes both above and below on the same probe) so data from this electrode was excluded from further analysis.

2.3. Soil Greenhouse Gas Measurements

To measure soil methane concentrations, we used soil gas sampling probes (following the protocol of *Dinsmore et al*. [2009]), which involved collecting gas phase samples from soils through a water-impermeable membrane. This allowed us to quantify the gaseous concentration of methane in equilibrium with the surrounding soil pore water. We chose this method so that we could collect data from both saturated and unsaturated soils along the length and depth of the transect, including stream sediments. Since the volume of water that the gas probe is in equilibrium with is not known, it is inappropriate to represent the value as an aqueous concentration, and we express the soil gas data as parts per million by volume (ppmv). The soil gas probes were constructed of 6 mm OD steel tubing (Swagelok, Solon, USA) and were inserted into the soil at depths of 0.1, 0.2, and 0.3 m, within 1 m distance of the redox probes. We inserted gas sampling probes to the maximum possible depth as the thaw front deepened (from a minimum of 0.08 m at the beginning of the thaw season to maximum 0.68 m at the end), until probes were situated at the target depths. We installed extra gas probes and sampled from the deepest possible depths (up to 0.68 m) at three locations: in the middle of the stream channel (near R1), on the edge of the stream channel (near R2), and at the uppermost position on the hillslope (near R9). The soil sampling probes were sealed at the bottom but had openings at a distance of 2.5 cm from the end of the probe which were covered by a 5 cm length of gas

permeable/water impermeable membrane (ACCUREL® PP V8/2 HF), which allows gases to diffuse into the tube without water ingress. The ACCUREL membrane was sealed to the probe using rubber paint (Plasti Dip®, Petersfield, UK), and the entire tube covered with white heat-shrink rubber tubing to minimize heat absorption by metal parts exposed to solar radiation. Prior to each sampling, a volume of air equal to the approximate internal volume of the probe was purged to the atmosphere. Suction was then applied to the tube using a 60 ml syringe for 48 h (72 h in September) then 20 ml of sample was injected into a 12 ml pre-evacuated gas-tight borosilicate Exetainer® vial (Labco, UK). Where less than a 20 ml volume of gas was collected over the sampling period, the remaining volume was made up to 20 ml in the laboratory using standard gas of known CO_2 and methane concentration, and sample concentrations calculated after analysis by mass balance:

$$C_S = \frac{C_M \times 20\ \text{ml} - C_D \times V_D}{V_S} \quad (1)$$

Where C is the concentration of either CO_2 or methane, and V the volume of respective gas fractions. Subscripts denote sample (S), dilution gas (D), and measured (M) concentrations and volumes, respectively.

We collected 184 gas samples in total, of which 112 contained more than 4 ml of sample. The samples were analyzed for CO_2 and methane concentrations using gas chromatography (Hewlett-Packard, HP5890, Series II gas chromatograph, fitted with two 2 m Hayes Sep Q columns (80–100 mesh) in series, and including a CO_2 methanization catalyst and flame ionization detector) at the University of Stirling, UK.

2.4. Stream Greenhouse Gas Concentrations

Dissolved methane and CO_2 gas samples ($n = 8$) were collected in the stream ~30 m downstream of the transect using the headspace technique [*Kling et al*., 1992; *Dinsmore et al*., 2013]. A 40 ml water sample was equilibrated with a 20 ml headspace of ambient air (collected from between 2 and 10 cm water depth) in a 60 ml syringe at natural stream temperature by shaking the syringe for 1 min vigorously underwater at the sampling point. Sampling depth was noted and used to calculate total (air plus water) system pressure, along with in situ field parameters (pH, electrical conductivity, EC, and temperature) using Hanna Instruments® HI-9033 and HI-9124 meters. The equilibrated headspace was then injected into a 12 ml preevacuated Exetainer® vial. Multiple ambient samples were collected and stored in Exetainer® tubes during sampling days. Both headspace and ambient samples were analyzed at the Centre for Ecology and Hydrology (CEH Edinburgh, UK) on an HP5890 Series II gas chromatograph (Hewlett-Packard) with flame ionization detector and attached methanizer. Detection limits for methane were 84 ppbv. Henry's Law was then used to calculate concentrations of CO_2 and methane dissolved in the stream water from the headspace and ambient concentrations [e.g., *Hope et al*., 1995]. Stream CO_2 and methane concentrations on one occasion (22 July) were not measured so were estimated from the relationship between CO_2 and methane concentrations ($\mu g\ L^{-1}$) and DOC at the same location (including four samples taken in early June and mid-September; data not shown) (methane versus DOC, $R^2 = 0.62$, $p < 0.01$, $n = 10$). Surface water samples for dissolved organic C (DOC) were collected using a 60 ml syringe from approximately 5 cm depth in the water column and the sample injected through 0.45 μm Millipore syringe-driven filters and stored without headspace in 30 or 60 ml bottles that were first rinsed with the filtered sample. Samples were kept cool (<6°C) and dark prior to analysis. The filtrate was analyzed for DOC concentration at CEH Edinburgh on a PPM LABTOC Analyzer (detection range of 0.1–4000 $mg\ L^{-1}$); concentrations were calculated based on a three-point calibration curve with a maximum of 50 $mg\ C\ L^{-1}$. Greenhouse gas concentrations are expressed as $\mu g\ L^{-1}$ (CH_4 or CO_2) or excess partial pressure ($epCH_4$), defined as the partial pressure of methane in solution divided by the partial pressure of methane in the atmosphere.

2.5. Other Field Measurements

We measured shallow groundwater levels during the thaw season using 2.5 cm diameter PVC piezometers at five positions (within 1 m of R3, R4, R6, R7, and R9), as well as the depth of the thaw front at each transect position, for each gas sampling event. Soil pH was also determined for each redox probe position and depth in the laboratory on field-moist soil (2:1 w/w soil: de-ionized water) collected using a 2.5 cm gauge corer.

Daily precipitation data were obtained from the nearby Environment Canada weather station ~320 m from our sampling location (Station ID: 220 N005; 68°44′46.8″N, 133°30′06.4″W).

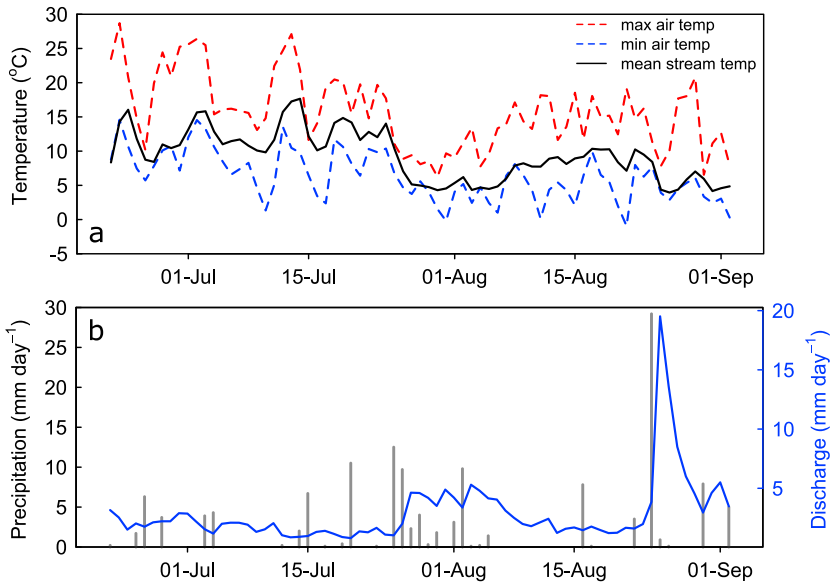

Figure 2. Meterological conditions during the study period: (a) Maximum and minimum daily air temperatures and average daily stream temperature, and (b) daily precipitation and stream water discharge for Siksik Creek (where a daily discharge of 10 mm d^{-1} is equivalent to an average daily discharge of 61.8 L s^{-1}).

2.6. Data Analysis

To test relationships between soil methane concentrations and redox conditions in the active layer, candidate models were compared using the leaps (v2.9) package in R (v3.1.2) [*R Core Team*, 2016]. This analysis involved an exhaustive search of all possible linear models including any or all of the following seven explanatory variables: soil depth (m), redox potential at time of sampling (Eh, mV), soil temperature (°C), active layer depth (m), water table depth (m), number of days (since soil thaw) that Eh < 200 mV (days), and date (DOY; day of year).

The best supported linear model was selected based on Akaike Information Criterion AIC, a criterion allowing model selection based on a trade-off between goodness of fit and model complexity which penalizes overfitting. Methane concentration data were $\log_{10}$ transformed prior to analysis.

To examine potential coupling between hillslope soils and stream water methane concentrations, Pearson correlations were calculated between stream water methane concentrations and hillslope soil methane concentrations at each soil depth and hillslope position. We had limited data from stream sediments at 0.3 m < depth < 0.5 m so data from these depths were grouped into a single depth category.

3. Results

3.1. Site Conditions

Weather conditions in July 2014 were generally warmer and drier than in August, with maximum daily air temperatures in July often exceeding 20°C (Figure 2a). There was a change in weather conditions from the end of July, with cooler air temperatures approaching freezing overnight. Stream temperatures also dropped from the end of July (mean daily temperature for July is 11.4°C) and were generally lower in August (mean daily temperature 7.3°C). The reduction in air temperature at the end of July was accompanied by an increase in precipitation and stream discharge (Figure 2b); average daily stream discharge for July was 1.9 mm d^{-1} and for August 3.9 mm d^{-1}. The largest single rain event occurred on 24 August at ~4 am, when 29 mm of precipitation fell over 24 h, equivalent to 50% of the total precipitation for July (Figure 2b). The extent of the saturated soil zone above the frost table was also greater in August/September (varying from 0 m at R3 to a maximum of ~0.38 m at R7) than in July (0 m at R3 to ~ 0.21 m at R7) (Table 1).

Thaw depth at the beginning of the measurement period was 0.10–0.19 m across the hillslope and channel bank, and 0.35 m in the stream channel. Thaw depths increased to a maximum value of 0.57 m on the

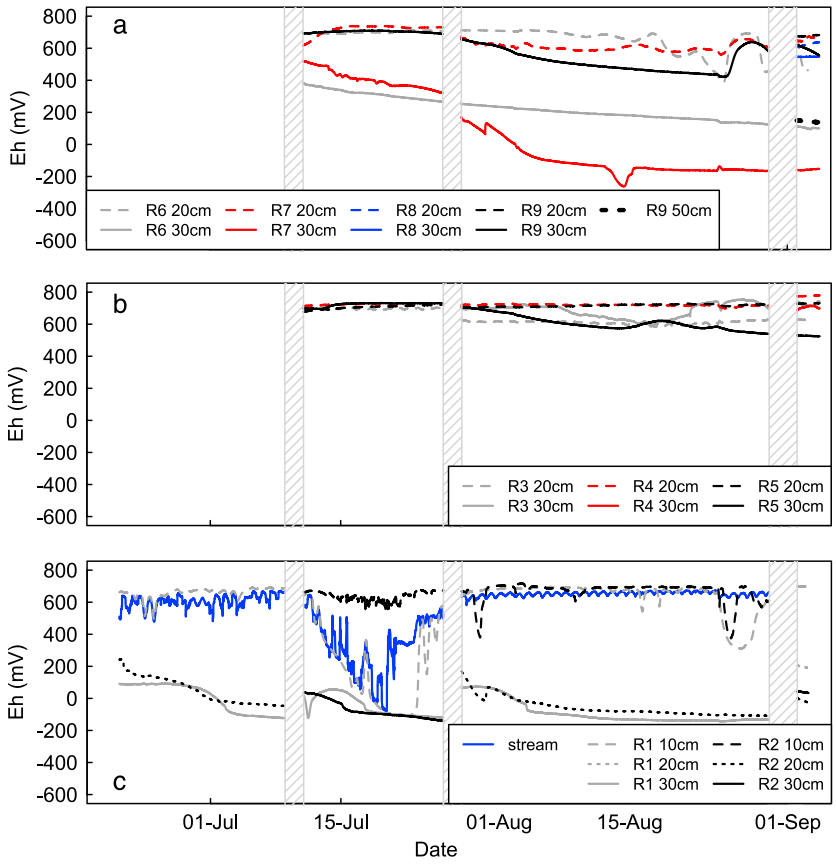

Figure 3. Redox potential (Eh) through time in (a) hillslope soils (probes R6–R9), (b) channel bank soils (probes R3–R5), and (c) in the stream water and stream channel sediments (probes R1 and R2). Hatched areas indicate time periods when redox probes were disturbed so no data are available. Eh at 0.1 m soil depth was > +600 mV throughout thaw season at all positions on the hillslope and, for clarity, these data are omitted from the figure.

hillslope (at R7) and 0.81 m in the stream channel (R1) by September (Table 1). The shallowest thaw depths by the end of the measurement period were at R3 (0.35 m) and R4 (0.41 m). The depth of the soil organic horizon was on average 0.16 m for R5–R9, but deeper at R3 and R4 on the lower hillslope where the depth of organic soil exceeded the maximum thaw depth. Sediments in the stream were highly organic to a depth of 0.1–0.2 m, but a dense root mat extended to depths >0.5 m in the center of the stream channel. Soil pH varied between 4.6 and 5.7; there was no clear pH trend with soil depth (Table 1).

3.2. Redox Dynamics in Hillslope Soils

Soil redox potentials (Eh) were greater than +400 mV at 0.1 m and 0.2 m depths across the hillslope and channel bank (R3–R9) for the duration of the growing season (Figures 3 and 4). There was a negative trend in Eh through time at the hillslope positions (R5–R9) at 0.3 m depth, and Eh values fell below +200 mV from the beginning of August onward at R6 and R7. Eh < +200 mV was also recorded at 0.5 m at R9 in early September (Figure 4). The lowest Eh values recorded in the hillslope soils were at R7 where Eh was <0 mV from 2 August onward (Figure 3a). On the channel bank at R3 and R4, Eh was > +600 mV at all profile depths throughout the thaw season (Figure 4), though data for R4 at 0.3 m were only available from the end of August (Figure 3b) because active layer depths were shallower at this position (Table 1). There was a simultaneous increase in Eh from ~+400 mV to +600 mV on 25 August around 0200 h at R6 (0.2 m) and R9 (0.3 m), which occurred following the large rain event on 24 August and also coincided with a significant increase in stream discharge (Figure 2b). Eh at these positions then began to decrease again after ~3 days (Figure 3a).

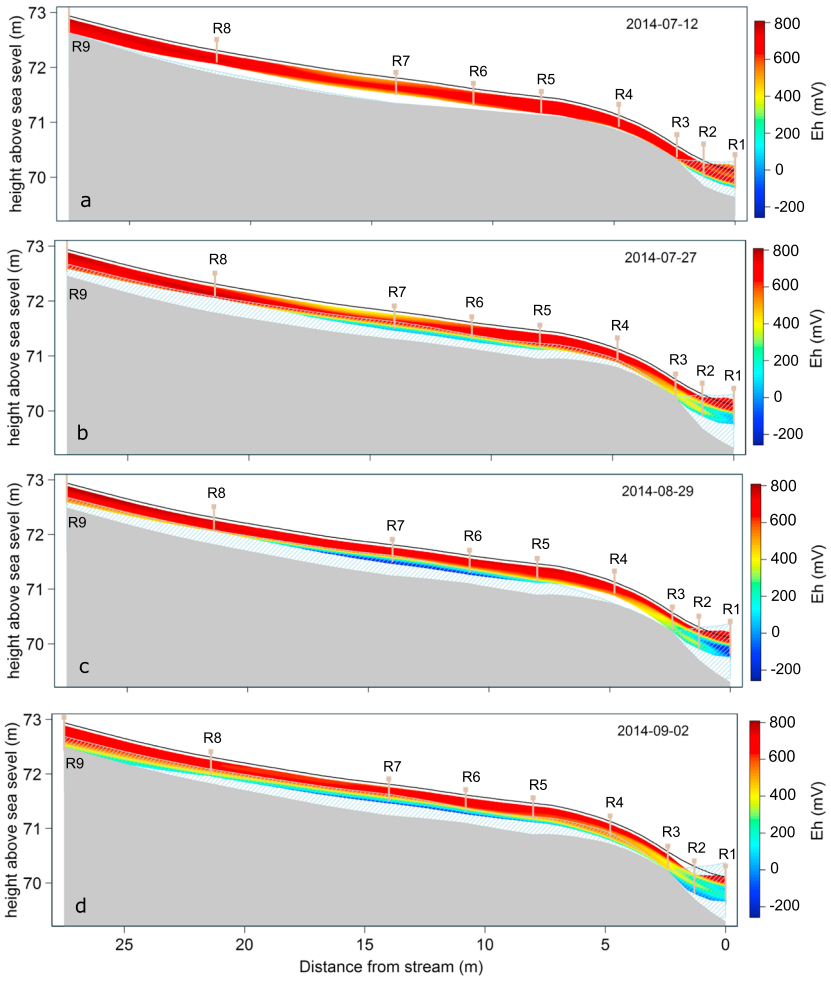

Figure 4. Spatial patterns of redox potential (Eh) along a transect perpendicular to Siksik Creek. (a–d) Data from four dates through the thaw season, 24 h prior to soil profile gas sampling (see Figure 5). Redox potentials (mV) are interpolated across a regular grid with respect to the ground surface using a loess smoothing function. The position and depth of the probes are indicated. The middle of the stream channel is at 0 m on the *x* axis. Blue cross-hatching indicates the position of the saturated soil zone based on piezometer data, grey represents frozen ground, white areas indicate no available data.

3.3. Redox Dynamics in Stream Water and Channel Sediments

Redox potential in the stream water and shallow sediments (0.1 m depth) varied between approximately +600 mV and −100 mV over the course of the thaw season (Figure 3c). In mid-July there was a period during which Eh was significantly lower in the midchannel stream water and shallow sediments (R1) than during the rest of the measurement period, eventually reaching negative values on 18 July (Figure 3c). Stream water and shallow sediment redox potentials then returned to values around +600 mV in early August, but Eh in the stream water recovered approximately 3.5 days earlier than in the sediment. On 24 August at approximately 0900, Eh in the stream sediments at 0.1 m decreased from approximately +650 mV to +350 mV then recovered over the next 3 to 4 days (Figure 3c). This decrease in Eh in the shallow sediments also occurred following the large precipitation event and subsequent spike in stream discharge, which began on the 24 August. Eh values for the deeper stream sediments (0.2 m and deeper), both in the midchannel (R1) and channel edge (R2), remained between −100 and +100 mV for the entire measurement period (Figures 3c and 4).

3.4. Greenhouse Gas Concentrations in Hillslope Soils and Channel Sediments

Average methane concentrations (in parts per million by volume, ppmv, subsequently denoted ppm) in upper organic hillslope soils (at 0.1 m depth) varied between 1.2 and 34 ppm. The highest methane

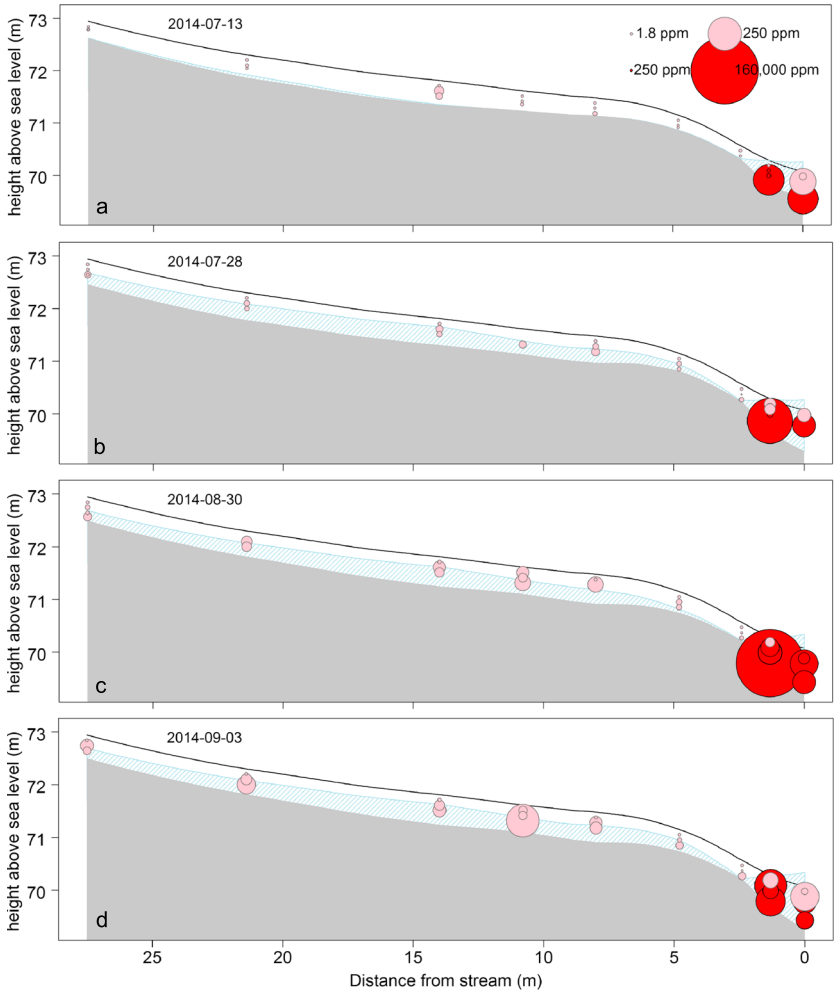

Figure 5. Soil methane concentrations along a transect perpendicular to Siksik Creek. (a–d) Data from four dates through the thaw season. The area of each circle is proportional to the measured concentration of methane (ppm). Pink symbols show data in the range 1.8–250 ppm, and red symbols show data in the range 250–160,000 ppm. Blue cross-hatching indicates the position of the saturated soil zone based on piezometer data, and grey represents frozen ground.

concentrations at 10 cm depth were measured on 30 August at R6 (17 ppm) and R7 (3.3 ppm) and on 3 September at R6 (34 ppm) and R7 (3.1 ppm) (Figure 5). At all other locations on the hillslope, soil methane at 0.1 m depth was on average 2.1 ± 0.05 ppm (comparable to atmospheric concentrations) over the duration of the thaw season. In general, soil methane concentrations increased over time and with depth in the profile (Figure 5). The exception was on the lower hillslope at R3, where average concentrations at 0.2 m depth (1.3 ± 0.15 ppm) were consistently lower than at 0.1 m (2.1 ± 0.02 ppm) and 0.3 m depth (7.9 ± 2.8 ppm). Methane concentrations in the stream bed sediments were several orders of magnitude higher than those in hillslope soils (Figures 5 and 6a). At ≥0.2 m depth methane concentrations in the stream sediments varied between 15 and 160,168 ppm. The highest concentration of 160,168 ppm (16.2% by volume) was measured on 30 August at R2 at 0.5 m depth (Figure 5c). At 0.1 m depth methane concentrations in the stream sediments varied between 1.5 and 54 ppm (Figure 5). CO_2 concentrations varied between 3628 and 528,000 ppm in the stream sediments, and between 483 and 154,000 ppm across the hillslope (Figure S3).

The best supported model of soil and sediment methane concentrations included four parameters: measurement depth, water table position, thaw depth, and number of days Eh < +200 mV. This model was able to explain 84% of the variability in log(CH_4 concentration) (Table 2). An identical model using redox potential immediately prior to measurement rather than the number of days Eh < 200 mV explained 76% of the variability in measured log(CH_4 concentration).

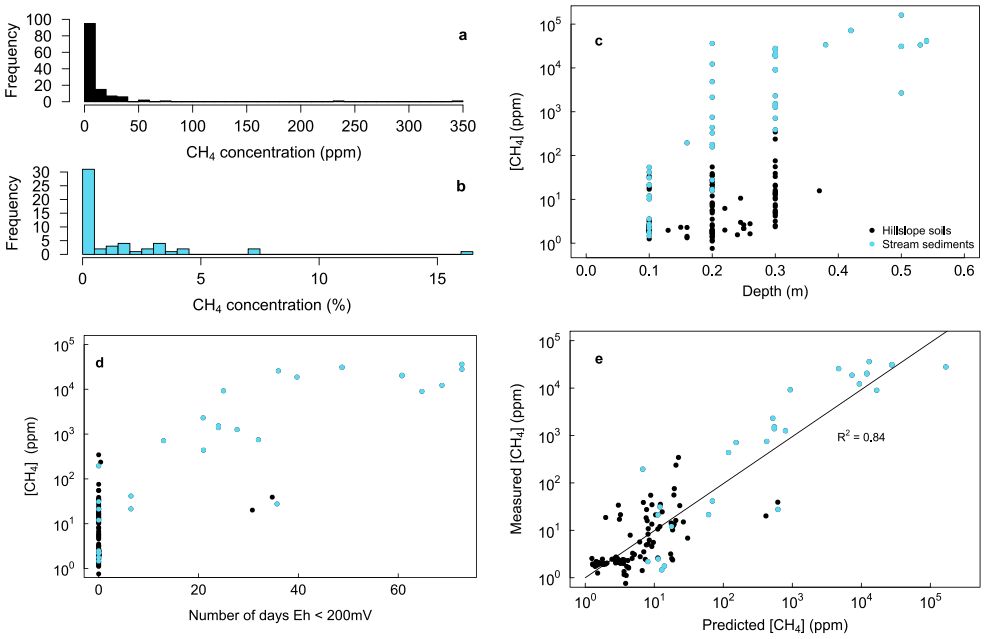

Figure 6. Soil and sediment methane concentrations and relationships with environmental variables: (a) Frequency distributions of methane concentrations for the hillslope and channel bank soils (R3–R9**),** (b) Frequency distributions of methane concentrations for the stream channel (R1 and R2) sediments, (c) relationship between soil/sediment methane concentrations and measurement depth, (d) relationship between soil/sediment methane concentrations and number of days Eh $<$ +200 mV, and (e) measured versus modeled methane concentrations, based on best supported linear regression model including measurement depth, number of anaerobic days (Eh $<$ +200 mV), water table depth, and thaw depth as explanatory variables.

3.5. Aquatic Methane Concentrations

Stream water methane concentrations varied between 1.4 and 11.7 $\mu g\,L^{-1}$ (50–490 μatm) between mid-June and early September (Figure 7a). These concentrations correspond to epCH_4 values of approximately 28–234. The highest recorded stream water methane concentrations occurred between 14 and 16 July when stream discharge was low. The lowest stream water methane concentrations occurred in late August and September (Figure 7a). All the stream water samples were taken during periods when redox potential in the water column was greater than +300 mV (Figure 7a), and there was no correlation between stream water redox potential and stream water methane concentrations.

Figure 7b shows a "heat map" of the strength of correlation between soil methane concentrations and stream water methane concentrations through time, for each distance from the stream and depth in the soil profile. There was some evidence of a positive association between stream water and soil methane concentrations at 0.2 m depth on the channel bank (R3), but in general, methane concentrations were negatively correlated with soil methane concentrations through time. These correlations were strongest in the midhillslope positions (Figure 7b).

Table 2. Results for Best Supported Multiple-Regression Model of $\log_{10}$ (CH_4 Concentration) for Active Layer Soils and Sediments[a]

Coefficients	Estimate	Std. Error
Soil Depth***	0.040	0.005
Active Layer Depth**	1.15	0.390
Water Table Depth***	−1.73	0.345
Days Eh $<$ +200 mV***	0.037	0.004

[a]Significance is indicated by ***$P < 0.001$ and **$P < 0.01$. Residual S.E. = 0.49 (124 df); Adjusted $R^2 = 0.84$; $F_{4,124} = 163.4$; $P < 2.2e{-}16$.

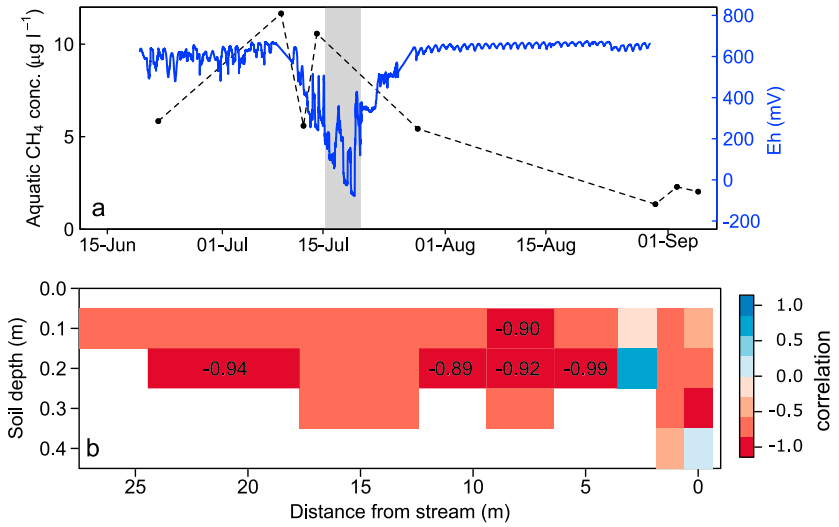

Figure 7. (a) Stream water methane concentrations through the thaw season plotted with stream water redox potential. The grey-shaded area indicates the time period during which stream redox potential was $< +200$ mV, and (b) heat map of correlations between soil methane concentration and aquatic methane concentrations at each position and soil depth on the transect. Where values are given, $p < 0.05$. Correlations are only shown where $n > 4$.

4. Discussion

4.1. How Do Redox Conditions in Hillslope Soils Vary Through the Thaw Season as the Active Layer Deepens?

Redox potentials varied between −200 and +700 mV, a typical range for soils under natural conditions [*Yu et al.*, 2007]. On the channel bank within 5 m of the stream, the organic horizon was deeper and the maximum thaw depth shallower than elsewhere on the transect; as a result the active layer soil profile consisted only of organic material. The expectation might be that these highly organic soils would more quickly generate reducing conditions [*Ponnamperuma*, 1972]; however, at these locations redox potentials were oxidizing at all depths because there was no persistent saturated soil zone above the permafrost table. The underlying topography of the permafrost, or the greater hydraulic conductivity of the organic soil, presumably promoted rapid drainage at this location (Figure 8). At distances greater than 5 m from the stream, saturated soils of 0.1 m to 0.3 m depth overlay the permafrost table for most of the thaw season; however, even where soils were saturated, it took time for reducing conditions to develop. The only hillslope locations where soils became strongly reducing were at R6, R7, and R9, but at these locations redox potential did decrease to less than +200 mV by the end of the thaw season.

By contrast, redox conditions at depth in the stream channel were strongly reducing from the beginning of the measurement period in mid-June. While it is possible that reducing conditions had developed rapidly early in the spring before measurements began, considering the slow trajectory of change in Eh further upslope, and the very high concentrations of methane observed early in the season, it is more likely that redox conditions remain reducing all year round at depth beneath the stream. Biological activity can continue in active layer soils over the winter [*Hultman et al.*, 2015] and may be significant beneath the stream bed where temperatures can remain close to 0°C [*Mikan et al.*, 2002] due to heat flux associated with running water [*Bradford et al.*, 2005]. Considering also that large quantities of root material were present at depth below the channel, providing a potential carbon substrate, year-round biological activity probably contributes to maintenance of reducing conditions throughout the year in the deeper stream sediments.

A simultaneous increase in redox potential of ~200 mV in soils at 20 cm depth at R6 and R7, and at 30 cm depth at R9, coincided with a major rain event on 24 August. Shifts in redox potential of this magnitude have previously been recorded in upland soils in response to precipitation events [*Mitchell and Branfireun*, 2005]. This increase may be caused by reduced groundwater being displaced by infiltrating oxygenated rain water, or by more oxygenated subsurface water through lateral flow from upslope. There was no response deeper in the soil profile at R6 and R7 to the same rain event, suggesting that downward vertical flow in these locations

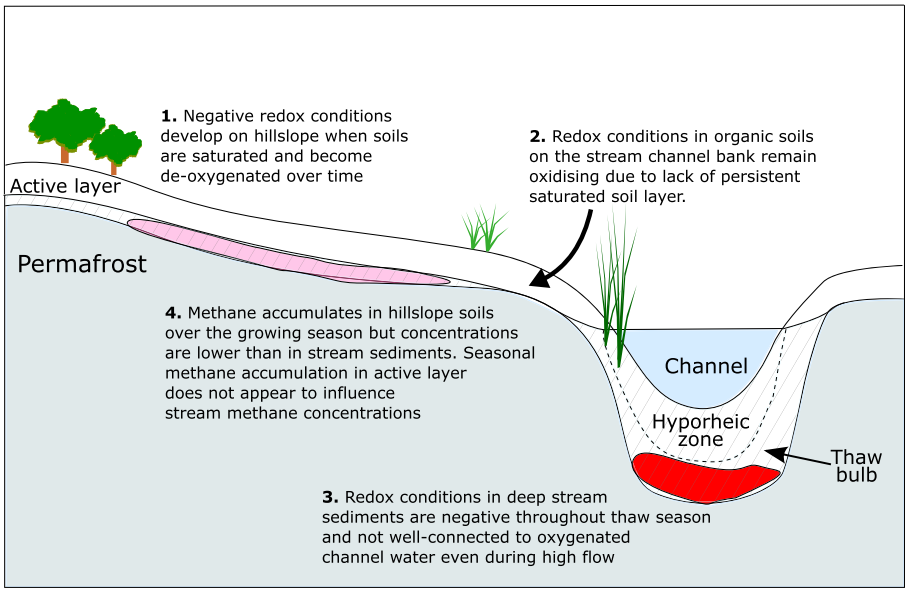

Figure 8. Conceptual model of hillslope redox processes. Hatched lines indicate saturated soils/sediments. The pink-shaded area indicates a transient zone of methane production which is dependent on reducing conditions developing over time during the thaw season. The red-shaded area indicates a permanently reducing environment with a zone of methane produced over multiple years.

was impeded or that the majority of the rainfall flowed overland or as shallow subsurface flow rather than in the deeper subsurface. This is consistent with previous work at the same site which has shown that near-surface peat soils provide less resistance to water movement than deeper layers, resulting in lateral water flow through near-surface soils [*Quinton et al*., 2000].

The presence of oxygenated conditions in the shallower stream sediments and water column showed that negative redox conditions can persist in the thaw bulb—thawed soils beneath the hyporheic zone [*Greenwald et al*., 2008]—probably because of limited exchange between the sediments and stream waters (Figure 8). This was true even under storm flow conditions in late summer—redox potentials did not respond in the deeper sediments to the rain event which occurred on 24 August. The decrease in redox potential in the shallower stream sediments at this time may indicate that under high flow conditions, there was an increase in the level of the less oxygenated groundwater below the stream bed; i.e., subsurface water was discharged toward the streambed as hillslope water was displaced, leading to a reduction in redox potential in the shallower sediments. An alternative explanation is that the upper hillslope becomes hydrologically connected and lateral flow from upslope soils into shallow organic sediments within the hyporheic zone temporarily impacts stream redox conditions; early stormflow is probably composed mainly of displaced pre-event soil water on the basis of evidence from other peat-dominated catchments [*Tetzlaff et al*., 2015].

4.2. How Are Redox Potentials in Hillslope Soils Related to Soil Methane Concentrations?

We observed elevated methane concentrations at depth in the hillslope soil profiles, with concentrations generally increasing over time through the season, as expected with the development of more negative redox conditions [*Fiedler et al*., 2007; *Yu et al*., 2007]. There was a clear positive relationship between methane concentrations and the amount of time for which redox potential in the soil or sediment was less than +200 mV; the duration of time for which reducing conditions were present was a better predictor of methane concentrations than instantaneous redox conditions at the time of measurement. This could be due to the buildup of methane over time in the soil, but could also reflect time lags inherent in the growth of methanogenic microbial communities once electrochemical conditions are favorable [*Lipson et al*., 2015] or the depletion of alternative electron acceptors such as NO_3^-, Fe(III), and SO_4^{2-} [*Peters and Conrad*, 1996]. Nitrate is unlikely to play a major role due to the low concentrations of nitrate found in soils at this site, even in vegetation dominated by *A. viridis* which is an N fixer (L. Street, unpublished data). Recent evidence also suggests

that organic matter can act as a terminal electron acceptor in temporarily anoxic environments which may also contribute to time lags in CH_4 formation [*Klüpfel et al*., 2014]. We found high concentrations of methane in the deep stream channel sediments throughout the thaw period. It is likely then that these high concentrations at depth in the early thaw season reflect methane production from previous years, including overwinter methane production [*Zimov et al*., 1997], concentrations having built up due to slow rates of transport through fine sediments, either via diffusion or ebullition [*Crawford et al*., 2014b].

As expected, negative redox potentials and enriched methane concentrations deeper in the soil profile indicate that the saturated zone above the permafrost table does provide conditions suitable for methanogenesis. Methane generation at depth in the soil profile does not necessarily result in a net methane efflux from the soil surface, as some or all of this methane may be oxidized in the surface layers [*Segers*, 1998, *Whalen and Reeburgh*, 1990], which we demonstrate had consistently oxidized redox potentials throughout the thaw season. The scope of this study did not include quantifying net terrestrial surface methane fluxes, but we did find evidence of significant methanotrophy within the organic soils on the channel bank, where concentrations of methane were below ambient atmospheric concentrations at 20 cm soil depth despite elevated concentrations in deeper soils. The stream surface does act as a net source to the atmosphere, however, as methane concentrations in the stream were consistently supersaturated with respect to atmospheric concentrations.

4.3. To What Extent Do Changing Active Layer Soil Conditions Influence Instream Redox Potential and Aquatic Methane Concentrations?

We found negative correlations between hillslope soil methane concentrations and the concentration of methane in the stream water. Negative correlations were a result of increases in methane concentrations in hillslope soils over time as negative redox potentials developed, while methane concentrations in stream water peaked in July, probably as a result of low discharge rates and warmer temperatures. Instantaneous stream water methane concentrations and hillslope soil methane concentrations were not correlated in this context, and in contrast to *Paytan et al*. [2015], groundwater discharge from the active layer did not appear to result in increased aquatic methane concentrations. The stream methane data are limited, however, and there may be time lags involved which were not possible to test due to a limited number of data points.

Methane concentrations in the deep stream bed sediments were several orders of magnitude higher than in hillslope soils. This raises the possibility that the processes determining methane transport from deeper, mineral stream sediments may be more important than lateral methane transport from hillslope soils in determining stream methane concentrations and efflux (Figure 8). These processes will include rates of diffusion and ebullition [*Wik et al*., 2014], and plant-mediated transport, as well as rates of methanotrophy in oxidized sediments or surface waters [*Schimel*, 1995]. Low stream discharge rates did result in strongly reducing redox conditions in the stream water for a week long period in July; this could potentially have dramatically reduced instream methane oxidation, and aquatic methane concentrations and surface fluxes may therefore have been higher. Unfortunately, our field campaigns did not coincide with the period when stream redox potentials were lowest, so we are unable to draw strong conclusions on the influence of stream redox conditions on stream water methane concentrations.

Spatial variability in the processes linking soil redox conditions and stream water biogeochemistry is likely to be high. Biogenic methane production in soils is highly spatially variable [*Moore et al*., 1990; *Wachinger et al*., 2000], and the processes mediating the transport of dissolved gases between the aquatic and terrestrial system also likely vary spatially along the length of the stream [*Waddington and Roulet*, 1997; *Hope et al*., 2004; *Crawford et al*., 2013]. We had no reason to believe that the transect was atypical, as it was situated between a common landscape unit (Alder shrub) and the stream bank, but we cannot generalize our results to the whole catchment on the basis of this single transect. The subcatchment of the transect was topographically linear, and while we find no evidence supporting the importance of terrestrial-aquatic methane transfer pathways in this particular case, this does not mean that these processes are never important. Concave subcatchment topographies, for example, may lead to increased biogeochemical influences from upslope [*Mitchell et al*., 2009]. However, our data do show consistent patterns in soil redox potential both through time and with soil (or stream) profile position, and we also show that redox conditions are strongly related to methane accumulation in soils. This study, therefore, provides a basis for further work which can test landscape-scale methane dynamics in more detail. For example, the use of an expanded grid or network of continuously

deployed redox probes could be used to interpolate spatial and temporal patterns in methane concentrations over larger scales. This kind of data is currently extremely challenging to obtain because of the need for intensive manual sampling in difficult and (often) remote terrain, but would allow for a much more comprehensive analysis of methane source areas, and the potential for lateral transfers of methane at the catchment scale.

4.4. Implications for Catchment Scale Methane Budgets

It was beyond the scope of this study to quantify methane evasion fluxes from along the length of Siksik Creek. However, we are able to provide context in terms of the aquatic contributions to methane fluxes at the catchment scale, based on the limited data available for other permafrost stream systems. *Crawford et al*. [2013] measured average fluxes during the open water season of between 0 and 80.5 mg CH_4 m^{-2} d^{-1} for streams within a headwater catchment of the Yukon River Basin, and estimate efflux from the stream network to account for up to ~10% of the terrestrial methane source strength. Measured $epCH_4$ values for streams in *Crawford et al*. [2013] varied between ~0.3 and ~4, which are low compared to values of 28–234 in this study. *Flessa et al*. [2008] report $epCH_4$ values between 54 and 1290 for streams at the forest-tundra ecotone in northern Siberia, but do not quantify evasion fluxes. In a catchment with sporadic permafrost in northern Sweden, *Lundin et al*. [2013] report epCH4 values between ~50 and ~1600 and corresponding mean methane fluxes from the stream surface which were high (253 mg CH_4 m^{-2} d^{-1}) compared to diffusive fluxes from lakes (12 mg CH_4 m^{-2} d^{-1}): Per unit catchment area, streams made an equivalent contribution to methane release as lakes, not including ebullition fluxes (around 0.1 g CH_4 m^{-2} yr^{-1}). We did not quantify terrestrial surface methane fluxes for the wider Siksik Creek catchment, but it is likely that for a significant fraction of the land surface corresponding to dwarf shrub/lichen dominated tundra, soils act as a small net sink for methane over the growing season (O. Sonnentag, personal communication, 2015).

4.5. Summary and Wider Implications

Figure 8 presents a conceptual model of the processes linking hillslope, redox conditions, and methane concentrations in soils and streams within the headwater catchment studied. Reducing conditions develop in active layer hillslope soils over the course of the growing season, but soil saturation conditions determine where and when reducing conditions develop (1). In this context, a zone of normally unsaturated organic soils exists at the edge of the stream channel (2) in which methane oxidation results in soil methane concentrations which are below atmospheric concentrations. Redox conditions in stream water and shallow stream sediments are usually oxidizing, but during periods of low flow can decrease to become strongly reducing. We also find evidence that precipitation events can influence both soil and stream redox conditions but only to a limited depth. High methane concentrations develop in stream sediments beneath the zone of hyporheic exchange (3). We find no evidence that increasing methane concentrations in the hillslope active layer during the growing season have an impact on methane concentrations in the stream water (4). Ebullition or diffusion from deeper stream sediments may therefore be more important than hillslope redox dynamics in determining aquatic methane fluxes under future climatic conditions. To our knowledge, this study is the first to explicitly examine the linkages between redox conditions in hillslope permafrost soils and headwater streams, and therefore provides important process-based information for an improved understanding of methane biogeochemistry under changing hydroclimatic regimes in a warming Arctic.

Acknowledgments
This work was funded by NERC grants NE/K000284/1 (P.A. Wookey), NE/K000225/1 (R. Baxter), NE/K000217/1 (M.F. Billett), and NE/K000268/1 (D. Tetzlaff) as part of the NERC Arctic Research Programme. We would like to thank the staff at the Aurora Research Institute, as well as Philip Marsh and Oliver Sonnentag, for providing logistical support. We also thank Philip Marsh and Oliver Sonnentag for assisting with access to long-term meteorological and hydrological information. Daily precipitation data for Trail Valley Creek are available from Environment Canada at http://climate.weather.gc.ca/. Data from the present study will be made available via the UK Environmental Information Data Centre (EIDC). Requests for access to the data should be directed to Philip Wookey (p.a.wookey@hw.ac.uk). We thank Ian Washbourne and Gwen Lancashire for their assistance with the fieldwork. We also thank three anonymous reviewers for their helpful suggestions in improving the manuscript.

References

Bastviken, D., L. J. Tranvik, J. Downing, P. M. Crill, and A. Enrich-Prast (2011), Freshwater methane emissions offset the continental carbon sink, *Science*, *331*, 50, doi:10.1126/science.1196808.

Baulch, H. M., P. J. Dillon, R. Maranger, and S. L. Schiff (2011), Diffusive and ebullitive transport of methane and nitrous oxide from streams: Are bubble-mediated fluxes important?, *J. Geophys. Res.*, *116*, G04028, doi:10.1029/2011JG001656.

Billett, M. F., and T. R. Moore (2008), Supersaturation and evasion of CO_2 and CH_4 in surface waters at Mer Bleue peatland, Canada, *Hydrol. Process.*, *22*, 2044–2054, doi:10.1002/hyp.

Bradford, J. H., J. P. McNamara, W. Bowden, and M. N. Gooseff (2005), Measuring thaw depth beneath peat-lined arctic streams using ground-penetrating radar, *Hydrol. Process.*, *19*(14), 2689–2699, doi:10.1002/hyp.5781.

Crawford, J. T., R. G. Striegl, K. P. Wickland, M. M. Dornblaser, and E. H. Stanley (2013), Emissions of carbon dioxide and methane from a headwater stream network of interior Alaska, *J. Geophys. Res. Biogeosci.*, *118*, 482–494, doi:10.1002/jgrg.20034.

Crawford, J. T., N. R. Lottig, E. H. Stanley, J. F. Walker, P. C. Hanson, J. C. Finlay, and R. G. Striegl (2014a), CO_2 and CH_4 emission from stream in a lake-rich landscape: Patterns, controls, and regional significance, *Global Biogeochem. Cycles*, *28*, 197–210, doi:10.1002/2013GB004661.

Crawford, J. T., E. H. Stanley, S. A. Spawn, J. C. Finlay, L. C. Loken, and R. G. Striegl (2014b), Ebullitive methane emissions from oxygenated wetland streams, *Global Change Biol.*, *1*, 3408–3422, doi:10.1111/gcb.12614.

Dean, J.F., Billett, M.F., Dinsmore K.J., Lessels, J., Street, L.E, Washbourne, I., Subke, J.A., Tetzlaff, D., Baxter, R. and Wookey, P.A. (2016), Biogeochemistry of "pristine" freshwater stream and lake systems in the western Canadian Arctic, *Biogeochemistry*, doi:10.1007/s10533-016-0252-2, in press.

Dinsmore, K. J., M. F. Billett, and T. R. Moore (2009), Transfer of carbon dioxide and methane through the soil-water-atmosphere system at Mer Bleue peatland, Canada, *Hydrol. Process.*, *341*, 330–341, doi:10.1002/hyp.

Dinsmore, K. J., M. F. Billett, and K. E. Dyson (2013), Temperature and precipitation drive temporal variability in aquatic carbon and GHG concentrations and fluxes in a peatland catchment, *Global Change Biol.*, *19*(7), 2133–2148, doi:10.1111/gcb.12209.

Fiedler, S., and M. Sommer (2000), Methane emissions, groundwater levels and redox potentials of common wetland soils in a temperate-humid climate, *Global Biogeochem. Cycles*, *14*(4), 1081–1093, doi:10.1029/1999GB001255.

Fiedler, S., M. J. Vepraskas, and J. L. Richardson (2007), Soil Redox Potential: Importance, Field Measurements, and Observations, in *Advances in Agronomy*, vol. 94, pp. 1–54, Elsevier Masson SAS, San Diego, Calif.

Flessa, H., A. Rodionov, G. Guggenberger, H. Fuchs, P. Magdon, O. Shibistova, G. Zrazhevskaya, N. Mikheyeva, O. A. Kasansky, and C. Blodau (2008), Landscape controls of CH_4 fluxes in a catchment of the forest tundra ecotone in northern Siberia, *Global Change Biol.*, *14*(9), 2040–2056, doi:10.1111/j.1365-2486.2008.01633.x.

Goncharuk, V. V., V. A. Bagrii, L. A. Mel'nik, R. D. Chebotareva, and S. Y. Bashtan (2010), The use of redox potential in water treatment processes, *J. Water Chem. Technol.*, *32*(1), 1–9, doi:10.3103/S1063455X10010017.

Greenwald, M. J., W. B. Bowden, M. N. Gooseff, J. P. Zarnetske, J. P. McNamara, J. H. Bradford, and T. R. Brosten (2008), Hyporheic exchange and water chemistry of two arctic tundra streams of contrasting geomorphology, *J. Geophys. Res.*, *113*, G02029, doi:10.1029/2007JG000549.

Grundl, T. (1994), A review of the current understanding of redox capacity in natural, disequilibrium systems, *Chemosphere*, *28*(3), 613–626, doi:10.1016/0045-6535(94)90303-4.

Hall, S. J., W. H. McDowell, and W. L. Silver (2012), When wet gets wetter: Decoupling of moisture, redox biogeochemistry, and greenhouse gas fluxes in a humid tropical forest soil, *Ecosystems*, *16*(4), 576–589, doi:10.1007/s10021-012-9631-2.

Hershey, A. E., R. M. Northington, J. Hart-Smith, M. Bostick, and S. C. Whalen (2015), Methane efflux and oxidation, and use of methane-derived carbon by larval Chironomini, in arctic lake sediments, *Limnol. Oceanogr.*, *60*(1), 276–285, doi:10.1002/lno.10023.

Hope, D., J. J. C. Dawson, M. S. Cresser, and M. F. Billett (1995), A method for measuring free CO_2 in upland streamwater using headspace analysis, *J. Hydrol.*, *166*(1–2), 1–14, doi:10.1016/0022-1694(94)02628-O.

Hope, D., S. M. Palmer, M. F. Billett, and J. J. C. Dawson (2004), Variations in dissolved CO_2 and CH_4 in a first-order stream and catchment: An investigation of soil–stream linkages, *Hydrol. Process.*, *3275*, 3255–3275, doi:10.1002/hyp.5657.

Hultman, J., et al. (2015), Multi-omics of permafrost, active layer and thermokarst bog soil microbiomes, *Nature*, *521*, 208–212, doi:10.1038/nature14238.

Husson, O. (2012), Redox potential (Eh) and pH as drivers of soil/plant/microorganism systems: A transdisciplinary overview pointing to integrative opportunities for agronomy, *Plant Soil*, *362*(1–2), 389–417, doi:10.1007/s11104-012-1429-7.

Jones, J. B., and P. J. Mulholland (1998), Methane input and evasion in a hardwood forest stream: Effects of subsurface flow from shallow and deep flowpaths, *Limnol. Oceanogr.*, *43*(6), 1243–1250, doi:10.4319/lo.1998.43.6.1243.

Kettunen, A., V. Kaitala, A. Lehtinen, A. Lohila, J. Alm, J. Silvola, and P. J. Martikainen (1999), Methane production and oxidation potentials in relation to water table fluctuations in two boreal mires, *Soil Biol. Biochem.*, *31*(12), 1741–1749, doi:10.1016/S0038-0717(99)00093-0.

King, J., and W. Reeburgh (2002), A pulse-labeling experiment to determine the contribution of recent plant photosynthates to net methane emission in arctic wet sedge tundra, *Soil Biol. Biochem.*, *34*, 173–180.

Kling, G., G. Kipphut, and M. Miller (1992), The flux of CO_2 and CH_4 from lakes and rivers in arctic Alaska, *Hydrobiologia*, *240*(1), 23–36, doi:10.1007/BF00013449.

Klüpfel, L., A. Piepenbrock, A. Kappler, and M. Sander (2014), Humic substances as fully regenerable electron acceptors in recurrently anoxic environments, *Nat. Geosci.*, *7*, 195–200, doi:10.1038/NGEO2084.

Knoblauch, C., O. Spott, S. Evgrafova, L. Kutzbach, and E. M. Pfeiffer (2015), Regulation of methane production, oxidation, and emission by vascular plants and bryophytes in ponds of the northeast Siberian polygonal tundra, *J. Geophys. Res. G Biogeosci.*, *120*, 2525–2541, doi:10.1002/2015JG003053.

Le Mer, J., and P. Roger (2001), Production, oxidation, emission and consumption of methane by soils: A review, *Eur. J. Soil Biol.*, *37*(1), 25–50, doi:10.1016/S1164-5563(01)01067-6.

Lipson, D. A., T. K. Raab, M. Parker, S. T. Kelley, C. J. Brislawn, and J. Jansson (2015), Changes in microbial communities along redox gradients in polygonized Arctic wet tundra soils, *Environ. Microbiol. Rep.*, *7*(4), 649–657, doi:10.1111/1758-2229.12301.

Lundin, E. J., R. Giesler, A. Persson, M. S. Thompson, and J. Karlsson (2013), Integrating carbon emissions from lakes and streams in a subarctic catchment, *J. Geophys. Res. Biogeosci.*, *118*, 1200–1207, doi:10.1002/jgrg.20092.

Marsh, P., C. Onclin, and N. Neumann (2002), Water and energy fluxes in the lower Mackenzie valley, 1994/95, *Atmos. Ocean*, *40*(2), 245–256, doi:10.3137/ao.400211.

McNicol, G., and W. Silver (2014), Separate effects of flooding and anaerobiosis on soil greenhouse gas emissions and redox sensitive biogeochemistry, *J. Geophys. Res. Biogeosci.*, *119*, 557–566, doi:10.1002/2013JG002433.

Medvedeff, C. A., and A. E. Hershey (2013), Importance of methane-derived carbon as a basal resource for two benthic consumers in arctic lakes, *Hydrobiologia*, *700*(1), 221–230, doi:10.1007/s10750-012-1232-8.

Mikan, C. J., J. P. Schimel, and A. P. Doyle (2002), Temperature controls of microbial respiration in arctic tundra soils above and below freezing, *Soil Biol. Biochem.*, *34*(11), 1785–1795, doi:10.1016/S0038-0717(02)00168-2.

Mitchell, C. P. J., and B. A. Branfireun (2005), Hydrogeomorphic controls on reduction-oxidation conditions across boreal upland-peatland interfaces, *Ecosystems*, *8*(7), 731–747, doi:10.1007/s10021-005-1792-9.

Mitchell, C. P. J., B. A. Branfireun, and R. K. Kolka (2009), Methylmercury dynamics at the upland-peatland interface: Topographic and hydrogeochemical controls, *Water Resour. Res.*, *45*, W02406, doi:10.1029/2008WR006832.

Moore, T., N. Roulet, and R. Knowles (1990), Spatial and temporal variations of methane flux from subarctic/northern boreal fens, *Global Biogeochem. Cycles*, *4*(1), 29–46, doi:10.1029/GB004i001p00029.

Parkin, T. B. (1987), Soil microsites as a source of denitrification variability, *Soil Sci. Soc. Am. J.*, *51*, 1194–1199, doi:10.2136/sssaj1987.03615995005100050019x.

Paytan, A., A. L. Lecher, N. Dimova, K. J. Sparrow, F. G.-T. Kodovska, J. Murray, S. Tulaczyk, and J. D. Kessler (2015), Methane transport from the active layer to lakes in the Arctic using Toolik Lake, Alaska, as a case study, *Proc. Natl. Acad. Sci. U.S.A.*, 201417392, doi:10.1073/pnas.1417392112.

Peters, V., and R. Conrad (1996), Sequential reduction processes and initiation of CH_4 production upon flooding of oxic upland soils, *Soil Biol. Biochem.*, *28*(3), 371–382.

Ponnamperuma, F. N. (1972), The chemistry of submerged soils, *Adv. Agron.*, *24*(C), 29–96, doi:10.1016/S0065-2113(08)60633-1.
Quinton, W. L., and J. W. Pomeroy (2006), Transformations of runoff chemistry in the Arctic tundra, Northwest Territories, Canada, *Hydrol. Process.*, *20*(14), 2901–2919, doi:10.1002/hyp.6083.
Quinton, W. L., and P. Marsh (1998), The influence of mineral earth hummocks on subsurface drainage in the continuous permafrost zone, *Permafrost Periglac. Process.*, *9*(3), 213–228, doi:10.1002/(SICI)1099-1530(199807/09)9:3<213::AID-PPP285>3.0.CO;2-E.
Quinton, W. L., and P. Marsh (1999), A conceptual framework for runoff generation in a permafrost environment, *Hydrol. Process.*, *13*(16), 2563–2581, doi:10.1002/(SICI)1099-1085(199911)13:16<2563::AID-HYP942>3.0.CO;2-D.
Quinton, W. L., D. M. Gray, and P. Marsh (2000), Subsurface drainage from hummock-covered hillslopes in the arctic tundra, *J. Hydrol.*, *237*, 113–125, doi:10.1016/S0022-1694(00)00304-8.
R Core Team (2016), R: A language and environment for statistical computing. R Foundation for Statistical Computing, Vienna, Austria. [Available at https://www.R-project.org/.]
Rabenhorst, M. C., W. D. Hively, and B. R. James (2009), Measurements of soil redox potential, *Soil Sci. Soc. Am. J.*, *73*(2), 668, doi:10.2136/sssaj2007.0443.
Rampton, V. (1987), Quaternary geology of the Tuktoyaktuk Coastlands, Northwest Territories, *Mem. 423, Geol. Surv. Canada*, 98.
Schimel, J. P. (1995), Plant transport and methane production as controls on methane flux from arctic wet meadow tundra, *Biogeochemistry*, *28*(3), 183–200, doi:10.1007/BF02186458.
Segers, R. (1998), Methane production and methane consumption: A review of processes underlying wetland methane fluxes, *Biogeochemistry*, *41*, 23–51.
Sepulveda-Jauregui, A., K. M. Walter Anthony, K. Martinez-Cruz, S. Greene, and F. Thalasso (2015), Methane and carbon dioxide emissions from 40 lakes along a north–south latitudinal transect in Alaska, *Biogeosciences*, *12*(11), 3197–3223, doi:10.5194/bg-12-3197-2015.
Seybold, C. A., W. Mersie, J. Huang, and C. McNamee (2002), Soil redox, pH, temperature, and water-table patterns of a freshwater tidal wetland, *Wetlands*, *22*(1), 149–158, doi:10.1672/0277-5212(2002)022[0149:SRPTAW]2.0.CO;2.
Skoog, D. A., D. M. West, F. J. Holler, and S. R. Crouch (1996), *Fundamentals of Analytical Chemistry*, 7th ed., Saunders College Publishing, Fort Worth, Tex.
Sparks, D. L. (2003), Redox Chemistry of Soils, in *Environmental Soil Chemistry*, pp. 245–265, Elsevier, San Diego, Calif.
Teare, C. (1998), Spatial and temporal patterns of chemical solute signals in sixteen small tundra streams of the Trail Valley Creek watershed in the Western Canadian Arctic, Simon Fraser University, Vancouver.
Teh, Y. A., and W. L. Silver (2006), Effects of soil structure destruction on methane production and carbon partitioning between methanogenic pathways in tropical rain forest soils, *J. Geophys. Res.*, *111*, G01003, doi:10.1029/2005JG000020.
Tetzlaff, D., J. Buttle, S. K. Carey, K. McGuire, H. Laudon, and C. Soulsby (2015), Flow pathways, storage and runoff generation in northern catchments: A review, *Hydrol. Process.*, *29*(16), 3475–3490, doi:10.1002/hyp.10412.
Treat, C., et al. (2015), A pan-Arctic synthesis of CH_4 and CO_2 production from anoxic soil incubations, *Global Change Biol.*, *21*, 2787–2803, doi:10.1111/gcb.12875.
Van Bochove, E., S. Beauchemin, and G. Thériault (2002), Continuous multiple measurement of soil redox potential using platinum microelectrodes, *Soil Sci. Soc. Am. J.*, *66*, 1813–1820, doi:10.2136/sssaj2002.1813.
Vorenhout, M., H. G. van der Geest, and E. R. Hunting (2011), An improved datalogger and novel probes for continuous redox measurements in wetlands, *Int. J. Environ. Anal. Chem.*, *91*(7–8), 801–810, doi:10.1080/03067319.2010.535123.
Wachinger, G., S. Fiedler, and K. Roth (2000), Variability of soil methane production on the micro-scale: Spatial, *Soil Biol. Biochem.*, *32*(8/9), 1121.
Waddington, J. M., and N. T. Roulet (1997), Groundwater flow and dissolved carbon movement in a boreal peatland, *J. Hydrol.*, *191*(1–4), 122–138, doi:10.1016/S0022-1694(96)03075-2.
Walter, K. M., S. A. Zimov, J. P. Chanton, D. Verbyla, and F. S. Chapin (2006), Methane bubbling from Siberian thaw lakes as a positive feedback to climate warming, *Nature*, *443*(7107), 71–5, doi:10.1038/nature05040.
Whalen, S. C., and W. S. Reeburgh (1990), Consumption of atmospheric methane by tundra soils, *Nature*, *346*(6280), 160–162, doi:10.1038/346160a0.
Wik, M., B. F. Thornton, D. Bastviken, S. MacIntyre, R. K. Varner, and P. M. Crill (2014), Energy input is primary controller of methane bubbling in subarctic lakes, *Geophys. Res. Lett.*, *41*, 555–560, doi:10.1002/2013GL058510.Received.
Wik, M., R. K. Varner, K. W. Anthony, S. MacIntyre, and D. Bastviken (2016), Climate-sensitive northern lakes and ponds are critical components of methane release, *Nat. Geosci.*, *2*, 99–106, doi:10.1038/ngeo2578.
Wrona, F. J., M. Johansson, J. M. Culp, A. Jenkins, J. Mård, I. H. Myers-Smith, T. D. Prowse, W. F. Vincent, and P. A. Wookey (2016), Transitions in Arctic ecosystems: Ecological implications of a changing hydrological regime, *J. Geophys. Res. G Biogeosci.*, *121*, 650–674, doi:10.1002/2015JG003133.
Yu, K., F. Böhme, J. Rinklebe, H.-U. Neue, and R. D. DeLaune (2007), Major biogeochemical processes in soils—A microcosm incubation from reducing to oxidizing conditions, *Soil Sci. Soc. Am. J.*, *71*(4), 1406, doi:10.2136/sssaj2006.0155.
Zimov, S. A., Y. V. Voropaev, I. P. Semiletov, S. P. Davidov, S. F. Prosiannikov, F. S. Chapin, M. C. Chapin, S. Trumbore, and S. Tyler (1997), North Siberian lakes: A methane source fueled by Pleistocene carbon, *Science*, *277*(5327), 800–802.